

1 **Trading water for carbon: Sustained photosynthesis at the cost of increased water loss**
2 **during high temperatures in a temperate forest**

3 **Anne Griebel^{1,2*}, Lauren T. Bennett³, Daniel Metzen^{1,4}, Elise Pendall¹, Patrick N.J. Lane⁴,**
4 **Stefan K. Arndt²**

5 ¹ Hawkesbury Institute for the Environment, Western Sydney University, Locked Bag 1797,
6 Penrith, NSW 2570, Australia

7 ² School of Ecosystem and Forest Sciences, The University of Melbourne, 500 Yarra Boulevard,
8 Richmond, VIC 3121, Australia

9 ³ School of Ecosystem and Forest Sciences, The University of Melbourne, 4 Water St, Creswick,
10 VIC 3363, Australia

11 ⁴ School of Ecosystem and Forest Sciences, The University of Melbourne, Parkville, VIC 3010,
12 Australia

13 *Corresponding author: Anne Griebel (a.griebel@westernsydney.edu.au)

14 **Key Points:**

- 15 • GPP of temperate eucalypts was sustained at the cost of increased water use during hot
16 periods, but both fluxes decreased during dry periods.
- 17 • WUE estimates for the same period differed up to two-fold depending on the way it was
18 calculated.
- 19 • Doubling of ecosystem respiration turned the forest from a net sink into a net source of
20 carbon during a longer heatwave.

21 **Abstract**

22 Forest carbon and water fluxes are often assumed to be coupled as a result of stomatal regulation
23 during dry conditions. However, recent observations have indicated increased transpiration rates
24 during isolated heat waves across a range of eucalypt species under experimental and natural
25 conditions, with inconsistent effects on photosynthesis (ranging from an increase to a near total
26 decline). To improve the empirical basis for understanding carbon and water fluxes in forests under
27 hotter and drier climates, we measured the water use of dominant trees, and the ecosystem-scale
28 carbon and water exchange in a mature temperate eucalypt forest over three summer seasons. The
29 forest maintained photosynthesis within 16% of peak photosynthesis rates during all conditions,
30 despite up to 70% reductions in canopy conductance during a 5-day heatwave. While carbon and
31 water fluxes both decreased by 16% on exceptionally dry summer days, GPP was sustained at the
32 cost of up to 74% increased water loss on the hottest days and during the heatwave. This led to
33 ~40% variation in ecosystem water use efficiency over the three summers, and ~two-fold
34 differences depending on the way water use efficiency is calculated. Furthermore, the forest
35 became a net source of carbon following a 137% increase in ecosystem respiration during the heat
36 wave, highlighting that the potential for temperate eucalypt forests to remain net carbon sinks
37 under future climates will depend not only on their potential to maintain photosynthesis during
38 higher temperatures, but also on responses of ecosystem respiration to changes in climate.

39 **1 Introduction**

40 A hotter and drier future is likely for many of Australia's ecosystems. Australia's mean annual
41 temperature has increased by 1 °C since 1910, temperature distributions have shifted towards
42 higher average monthly maximum and minimum temperatures, and the duration, frequency and
43 intensity of extreme heat events has increased (BOM 2016a). The years 2013-2015 were among
44 the top 10 hottest years on record, including a number of significant heatwaves in southeast
45 Australia (BOM 2013, 2014, 2015). In addition, southeastern Australia has become drier due to
46 severe rainfall deficiencies since the year 2000 (BOM 2016b). This indicates increased potential
47 for climate-induced stress in Australian ecosystems, given projections of warmer and drier
48 conditions over much of the Australian continent in coming decades (IPCC 2013). This will likely
49 result in more hot days and fewer cool days, in addition to more time spent in drought as winter
50 and spring rainfall is predicted to decrease further (BOM 2016a).

51 Over 900 eucalypt species occur in a broad range of climates in Australia, some with relatively
52 narrow distributions, which could make them vulnerable to a changing climate (Brouwers et al.,
53 2013; Hughes et al., 1996; Jurskis, 2005), and especially to extreme climate events (Choat et al.,
54 2012; Matusick et al., 2013; Mitchell et al., 2014a). Many eucalypt species close their stomata to
55 prevent excessive water loss in response to dry conditions (Breshears et al., 2013; Eamus et al.,
56 2008), which delays embolisms in the stem xylem (Choat et al., 2012; Tyree & Sperry, 1989) at
57 the cost of decreases in photosynthesis and increases in the vulnerability of leaves to heat and light
58 stress (McDowell et al., 2008; McDowell, 2011; Mitchell et al., 2014b; Thomas & Eamus, 1999;
59 Whitehead & Beadle, 2004). Stomatal conductance varies with supply and demand for CO₂ by
60 photosynthesis (intercellular CO₂ concentration), leaf irradiance and leaf temperature, as well as
61 atmospheric vapor pressure deficit and leaf turgor (Ball et al., 1987; Cowan, 1978; Medlyn et al.,

62 2011; Tuzet et al., 2003). Hence, photosynthesis, transpiration and stomatal conductance are
63 commonly assumed to be coupled; that is, photosynthesis and transpiration both decrease with
64 increasing stomatal regulation under most environmental conditions (Farquhar & Sharkey, 1982;
65 Leuning, 1995; Tuzet et al., 2003). However, isolated studies provide evidence of a decoupling of
66 photosynthesis from stomatal conductance in some tree species during extreme heat stress (Ameye
67 et al., 2012; De Kauwe et al., 2019; Drake et al., 2018; Urban et al., 2017). For example,
68 photosynthesis decreased in seven eucalypt forests (De Kauwe et al., 2019) or was near zero in 1-
69 year-old *E. parramattensis* saplings (Drake et al., 2018) as water loss increased under high
70 temperatures. This indicates that latent cooling of leaves by transpiration might be an important
71 mechanism to cope with extended heat stress (Drake et al., 2018), in turn affecting the plant's
72 carbon assimilation rate per unit stomatal conductance as well as the plant's water use efficiency
73 (WUE). Nonetheless, in other temperate forest types dominated by eucalypts, photosynthesis
74 increased with transpiration during a single heat wave event (van Gorsel et al., 2016), highlighting
75 the need for further studies of concurrent carbon and water fluxes across an extended range of
76 weather conditions.

77 Individual studies of transpiration cooling under heat stress have largely focused on young plants
78 (Ameye et al., 2012; Drake et al., 2018; Urban et al., 2017), whereas direct measures of stomatal
79 conductance, carbon assimilation (GPP) and transpiration at the ecosystem level remain
80 challenging. Canopy conductance (G_c , as an approximation of stomatal conductance) is commonly
81 derived by inverting the Penman-Monteith equation using directly measured latent heat flux (LE;
82 Monteith, 1965). WUE has been estimated as the sum of GPP over the sum of ET, but this does
83 not account for the non-linear response of LE to vapor pressure deficit (VPD). Thus, alternative
84 formulations of ecosystem-scale WUE as underlying WUE (Zhou et al., 2015, 2014), or as intrinsic

85 WUE (Beer et al., 2009; Lloyd et al., 2002; Schulze and Hall, 1982) have been suggested to more
86 accurately understand the underlying physiological mechanisms.

87 Studies examining concurrent carbon and water fluxes under heat stress in natural mature eucalypt
88 forests are limited to isolated heatwave events (De Kauwe et al., 2019; van Gorsel et al., 2016).
89 Further, it remains unclear if eucalypts respond differently to multi-day heatwaves compared with
90 individual hot days, and how such responses might be mediated by water availability. As this is
91 currently neither well understood, nor integrated into process-based ecosystem models, it limits
92 the potential to predict how future climates characterized by more frequent and intense heatwaves
93 will influence the physiology, productivity, and distribution of temperate forest eucalypts. We
94 combined three years of concurrent sap flow and eddy covariance summer measurements in a
95 natural temperate eucalypt forest to examine the dynamics of photosynthesis and water use during
96 the hottest days, the driest days, and a 5-day heatwave. We hypothesized that (i) photosynthesis
97 and transpiration would both decrease on the driest days and both increase on the hottest days
98 (assuming no water limitations); and (ii) a longer heatwave would result in decreased carbon
99 uptake and increased water loss, as photosynthesis decreases, and evapotranspiration increases
100 during continuous temperature stress (assuming no water limitations). Our results have globally
101 relevant implications for understanding the trade-offs between photosynthesis and water use from
102 terrestrial ecosystems during exceptionally hot or dry conditions, which remain yet to be
103 incorporated into plant hydraulic and land surface models.

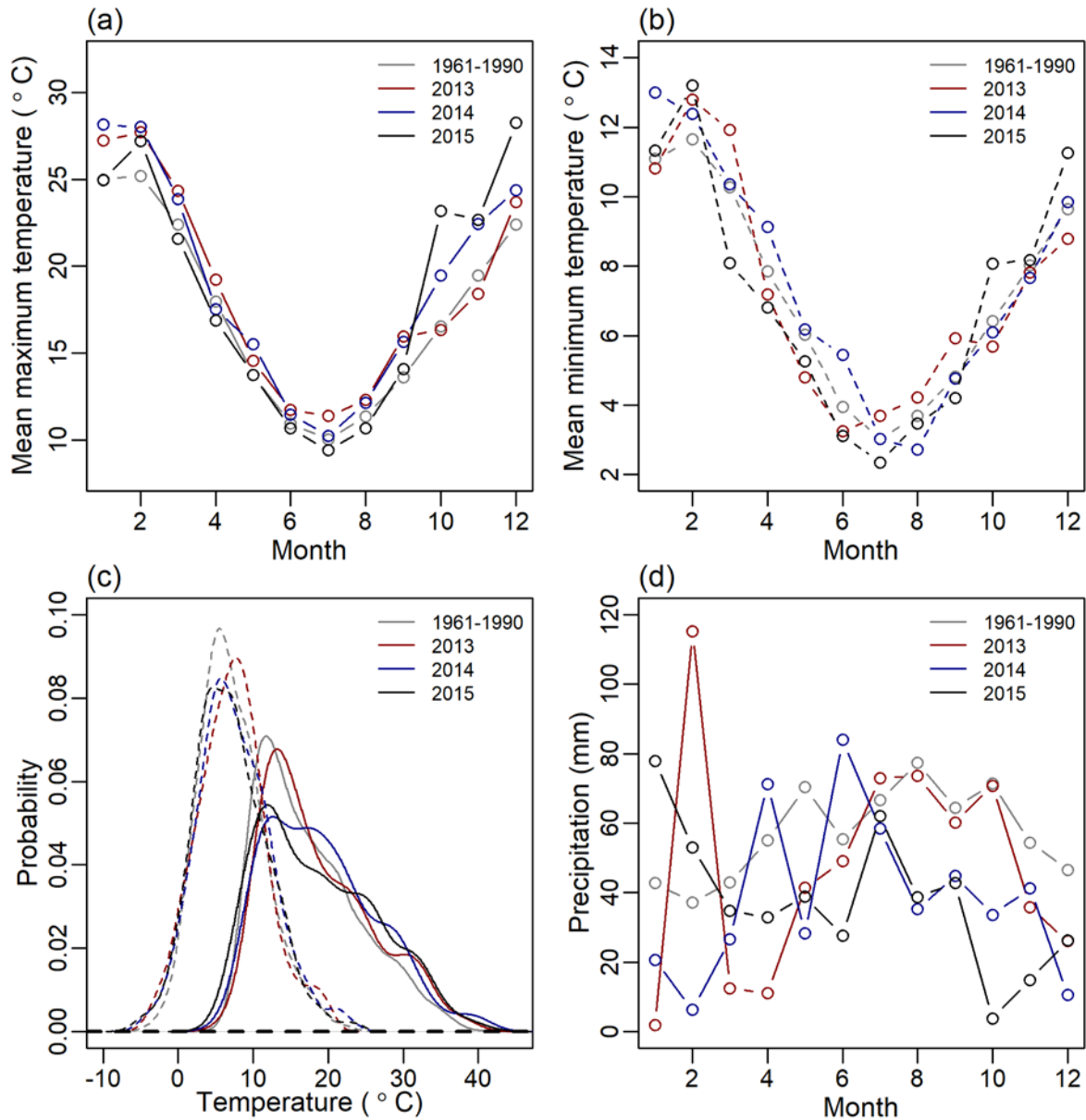
104 **2 Materials and Methods**

105 2.1 Study site and climate

106 We recorded tree water use and ecosystem carbon and water fluxes in a temperate mixed-species
107 eucalypt forest (Wombat State Forest) in southeastern Australia from January 2013 to November
108 2015. The study site is located near a ridge at 705 m elevation with gently sloping terrain to the
109 southwest and northwest ($< 8^\circ$; Griebel et al., 2016), approximately 100 km west of Melbourne,
110 Australia, and is part of the TERN-SuperSite Network, TERN-OzFlux and FluxNet (AU-Wom),
111 Sapfluxnet (AUS-WOM) and Dendroglobal network (AU-Wombat). Active forest management
112 has been minimal since the late 1970s, with previous management practices including selective
113 harvesting, low-intensity prescribed burning and firewood collection. The overstorey of this dry
114 sclerophyll forest is dominated by three eucalypt species: *Eucalyptus obliqua* L'Hér (deep fibrous
115 'stringybark'), *E. rubida* H. Deane and Maiden (smooth 'gum' bark), and *E. radiata* Sieber ex DC
116 (short fibrous 'peppermint' bark; 70%, 21% and 9% of stand biomass, respectively; Griebel 2016),
117 while the understory consists of sparse and patchy perennial grasses and the fern Austral bracken.
118 The leaf area index (LAI, acknowledging that it includes leaves and woody biomass) was relatively
119 stable in the first half of the study period (LAI $\sim 1.7 \text{ m}^2 \text{ m}^{-2}$), and subsequently increased by $\sim 20\%$
120 by the end of the study period (Griebel et al., 2017).

121 The climate is cool temperate, with typically cool and wet winters, and warm summers. The closest
122 weather station to the study site (Ballarat Aerodrome, ~ 20 km distance) recorded a long-term
123 average annual temperature of 12.2°C and an average annual rainfall of 690 mm (1908-2015).
124 While the mean annual temperatures of the three study years were slightly below the long-term
125 average (12.0°C in 2013, 11.8°C in 2014 and 10.8°C in 2015), mean monthly maximum and
126 minimum temperatures were generally greater than the World Meteorological Organization

127 (WMO) reference period (1961-1990) in spring and summer (baseline based on Ballarat
128 Aerodrome data; Fig. 1a,b). Likewise, probability distributions of the mean monthly minimum and
129 mean monthly maximum temperatures indicated a high likelihood for warmer temperatures during
130 each study year (Fig. 1c). The annual rainfall totals were within 90 mm of the long-term average
131 of 690 mm (780 mm in 2013, 672 mm in 2014 and 679 mm in 2015), but the 2014 and 2015
132 monthly rainfall totals were consistently below the WMO reference totals in winter and spring
133 (Fig. 1d).



134

135 **Figure 1.** Mean monthly maximum (a) and minimum (b) temperatures in spring (months 9 to 11)
136 and summer (months 1,2 and 12) were often higher during the three observation years than the
137 WMO reference period (1961-1990). This affected the likelihood of higher maximum
138 temperatures (solid lines, panel c) and to a lesser degree higher minimum temperatures (dashed
139 lines). Rainfall distribution (monthly rainfall totals, d) during the three years was erratic during
140 summer and autumn, but below average conditions in winter and spring in 2014 and 2015.

141 One of southeast Australia's most significant heatwaves (i.e. up to 12 °C higher than the 1961-
142 1990 January mean maximum; BOM 2014) coincided with our study period in January 2014, and
143 involved five consecutive days reaching ~35 °C and a peak vapor pressure deficit (VPD) of 5.4
144 kPa at our study site. Thus, all references to heatwaves in this paper refer to this local heatwave
145 ('HW', 13 to 17 January 2014), rather than the broader-scale 'Angry summer' of 2013 (van Gorsel
146 et al., 2016), which affected much of southeastern Australia but was comparatively mild at our
147 study site due to the >700 m elevation (i.e. isolated days with maximum temperatures in the low
148 30s °C).

149 Since the 2014 heatwave was preceded by numerous rain events at the end of 2013 (i.e. was hot
150 but well-watered), we also pooled the hottest and driest days throughout the summer months
151 (December to February 2013-2015) for comparison with the 5-day heatwave. Here, the hottest
152 days were those in the upper 90th percentile of maximum daily temperatures in summer (>30.7
153 °C; 19 days), and the driest days were those in the lowest 10 percent of summer dryness as
154 indicated by soil moisture sensors at 40 cm depth (<0.102 m³ m⁻³; 23 days). The 19 hottest days
155 excluded the heatwave from 13 to 17 January 2014 and did not overlap with any of the 23 driest
156 days. Note that soil moisture sensors at greater depths (65 cm, 1m; see 'Climate variables and
157 response functions') were installed too late to capture all summer months. In addition to the WMO
158 1961-1990 baseline, we defined a local January baseline ('Base'; 59 unique days) as days in
159 January 2013, 2014 and 2015 that excluded unusual weather conditions during part of the 'Angry
160 summer' from 1 to 19 January 2013, the heatwave from 13 to 17 January 2014, as well as the
161 hottest and driest 10% of days. The incoming solar radiation was comparable between the three
162 groups (Table 1 and Fig. S1), and the soil moisture was comparable during the baseline, the hottest
163 days and the heatwave. Thus, apart from the driest days (which were warm and dry), the four

164 groups primarily differed in their temperature range and associated atmospheric demand (which
165 increased from the baseline to the driest days, the hottest days, and peaked during the heatwave;
166 Table 1).

167 2.2 Sap flow measurements

168 Sap velocity (v_{sap}) was monitored half-hourly from 1 January 2013 to 31 October 2015 in eleven
169 trees: six *E. obliqua* (mean diameter at breast height, DBH = 41 cm, range 30.8 - 50.9 cm), and
170 five *E. rubida* (mean DBH = 33.3 cm, range 22.8 - 46.7 cm). All trees were healthy and all canopies
171 had access to direct sunlight. Crown class as identified by canopy position (Smith et al., 1997) was
172 evenly distributed between species, with two intermediate and three sub-dominant trees per
173 species, and one dominant *E. obliqua* (no dominant *E. rubida* were present). We utilized the heat
174 pulse compensation method to monitor sap velocity (The HeatPulser, Edwards Industries, Taupo,
175 NZ), and distributed four probes per tree with increasing implantation depth to cover the sap
176 velocity gradient (mean sapwood depth: *E. rubida* 1.95 ± 0.42 cm; *E. obliqua* 1.92 ± 0.38 cm).
177 Sap velocity was corrected for deviations from exact parallel spacing of the heater and the
178 thermistor elements, and wounding size was determined for all probes at the end of the study
179 period. In addition, tree cores were collected next to each probe to correct measured v_{sap} for the
180 individual gas and water fractions of the sapwood of each instrumented tree (Edwards and
181 Warwick 1984). Sap velocities were calculated for each probe and then averaged per tree. Each
182 probe was analyzed for velocity drifts relative to the other three probes per tree, and affected probes
183 were excluded from the analysis (2 probes in total). Data gaps through intermittent probe failures
184 were filled with a hierarchical system to avoid an offset in the signal if either the fastest or slowest
185 sensors were not working: 1. Gaps of individual probes were filled based on the highest fit of a
186 regression between the probe that needed filling and the other three probes in the same tree (a

187 probe was only chosen when $R^2 > 0.5$). If the fit with any probe of the same tree was below the
188 threshold, then the best fit with a probe from all other trees was chosen to fill the gap. 2. The v_{sap}
189 means of each tree were gap-filled if there were periods with a data gap affecting all probes of a
190 tree simultaneously (e.g. during a power outage, during data downloads or sensor repairs). Here,
191 we correlated the means of all trees with each other and chose the tree with the best fit. The lowest
192 correlation between two trees had a Pearson R of 0.85, so no minimum threshold had to be applied.

193 2.3 Eddy covariance measurements

194 We monitored ecosystem-scale carbon and water exchange from a flux tower adjacent to the trees
195 that were monitored for v_{sap} dynamics. Fluxes were recorded at 30 m height with an open-path
196 CO_2/H_2O analyzer (LI-7500, LI-COR Biosciences, Lincoln, NE, USA) and a 3-D sonic
197 anemometer (CSAT3, Campbell Scientific Inc., Logan, UT, USA), sampled at 10 Hz and averaged
198 over 30 minute intervals. Flux data were processed with ‘OzFluxQC’ version 2.9.5
199 (<https://github.com/OzFlux/OzFluxQC>), which included outlier removal through de-spiking, 2D
200 co-ordinate rotations, WPL correction (Webb et al., 1980), conversion of virtual to sensible heat
201 flux, and linear corrections for calibration anomalies and sensor drift (Griebel et al., 2017). We
202 used the built-in neural network from OzFluxQC (SOLO; Isaac et al., 2017) for gap-filling of
203 meteorological variables and fluxes. Data gaps of up to three hours were filled using linear
204 interpolations, while longer gaps were filled with a descending preference of using alternative
205 weather station data (Ballarat Aerodrome, ca. 20 km from study site), ACCESS model output from
206 the Bureau of Meteorology, and BIOS2 model output, and lastly, using site-specific half-hourly
207 averages of monthly climatology data (Isaac et al., 2017). We used 90-day intervals to gap-fill
208 drivers and monthly intervals to gap-fill fluxes. Fluxes of carbon, water, and latent and sensible
209 heat were gap-filled using incoming shortwave radiation, specific humidity deficit, and soil

210 temperature as independent variables. Year-specific friction velocity thresholds were determined
211 with the change-point detection method using 1000 iterations following Barr et al. (2013), which
212 were subsequently applied for partitioning of net ecosystem exchange (NEE) into gross primary
213 productivity (GPP) and ecosystem respiration (ER). Here, the neural network was trained with soil
214 temperature and soil moisture as independent variables, before ER was predicted across a range of
215 conditions that cover the entire data set of flux tower measurements. GPP was derived as $GPP = -$
216 $NEE + ER$, where $-NEE = NEP$ (net ecosystem productivity). We converted the gap-filled latent
217 heat flux (Wm^{-2}) to evapotranspiration (ET; mm) and daily means of water use efficiency (WUE)
218 were derived as $WUE_{day} = \sum GPP / \sum ET$ ($g C kg H_2O^{-1}$; Table 1). Further, we calculated the daily
219 mean underlying $WUE_{u_day} = GPP \times VPD^{0.5} / ET$ ($gC kPa^{-0.5} kgH_2O^{-1}$) to account for the non-linear
220 effect of increasing VPD on LE (Zhou et al., 2015, 2014) and the daily mean intrinsic $WUE_{i_day} =$
221 GPP / G_c ($gC mol^{-1} m^{-2} s^{-1}$) to quantify photosynthesis in relation to conductance (Beer et al., 2009;
222 Lloyd et al., 2002; Schulze and Hall, 1982).

223 We calculated canopy conductance (G_c ; $mol m^{-2} s^{-1}$) and potential evapotranspiration (PET; mm)
224 following Monteith (1965), where we used site-specific meteorological observations from the flux
225 tower measurements as input parameters, and identified the well-watered reference surface
226 conductance as the average of the surface conductance when VPD was between 0.9 and 1.1 kPa
227 and surface soil moisture exceeded the 75% quantile. To account for the energy imbalance when
228 inverting the Penman-Monteith equation to calculate canopy conductance and PET (Knauer et al.,
229 2018; Wilson et al., 2002), we set the available energy equal to the sum of the latent and sensible
230 heat flux, which implicitly conserves the Bowen ratio (Wohlfahrt et al., 2009). Rainy periods were
231 excluded from the analysis, and half-hourly data were resampled to hourly periods to reduce noise.

232 2.4 Climate variables and response functions

233 In addition to fluxes, we measured the following meteorological variables above the canopy:
234 downwelling and upwelling, shortwave and thermal radiation (CNR1; Kipp and Zonen, Delft, The
235 Netherlands), air temperature and relative humidity (Vaisala HMP155; Vaisala, Helsinki, Finland).
236 Precipitation was recorded as half-hourly totals at 1 m below the canopy (TB6; Hydrological
237 Services Pty Ltd, Warwick Farm, Australia), and we added an additional rain gauge of the same
238 type above the canopy in July 2014. Soil moisture measurements were initially recorded only at
239 10 and 40 cm depth close to the flux tower using time-domain measurement method to calculate
240 soil volumetric water content (CS-616; Campbell Scientific Inc., Logan, UT, USA), and we
241 extended these measurements by three additional sites adjacent to instrumented trees in November
242 2013. Thereafter, each of the four sites contained a CS-650 at 10 cm depth (Campbell Scientific
243 Inc., Logan, UT, USA) and three additional CS-616 at 40 cm, 65 cm and ca. 1 m depth (depending
244 on soil texture), and measurements from the four pits were averaged for each depth. We used one-
245 way ANOVAs followed by a Tukey test to assess significant differences in the response and key
246 climate variables between the baseline, the driest and the hottest days and heatwave days. All data
247 were analyzed in R version 3.5.1 (R Core Team, 2018) using the packages ‘dplyr’ and ‘reshape2’
248 for manipulations, and ‘car’ for statistical analyses.

249 **3 Results**

250 3.1 Trade-offs between water loss and carbon gain

251 The daily sums of v_{sap} , ET, GPP and daily means of WUE differed significantly among the baseline
252 days, the hottest and the driest days, and during the heatwave ($P < 0.01$; Table 1). However, no
253 variable was significantly different between the hottest days and the heatwave (Table 1),
254 suggesting that the eucalypts did not respond differently to the longer heatwave compared with the

255 individual hot days. On the driest days, v_{sap} of both species remained comparable to the baseline,
256 whereas v_{sap} increased by >45% during the hottest days and by >70% during the heatwave (Table
257 1). Daily ET patterns resembled v_{sap} patterns, indicating that transpiration dominated the ET signal
258 of this forest. Daily GPP was comparable between baseline days, the hottest days and during the
259 heatwave, but was significantly reduced during the driest days (16% lower than the baseline days;
260 Table 1). However, daily ER relative to the baseline increased by 36% during the driest days,
261 doubled during the hottest days, and increased by 137% during the heatwave (resulting in
262 significant differences among all groups with the exception of the hottest and heatwave days; Table
263 1). This led to significant reductions in daily NEE relative to the baseline, which were in the order
264 of 62% on the driest days, and 91% on the hottest days, and turned the forest from a moderate
265 carbon sink to a carbon source (positive NEE) during the heatwave (Table 1).

266 Mean daytime canopy conductance relative to the baseline decreased significantly when soil
267 moisture decreased (44% decrease in G_c during driest days with comparable mean daytime VPD;
268 Table 1), and decreased further when VPD and temperatures increased during the hottest days and
269 the heatwave (71% decrease in G_c despite comparable soil moisture to the baseline, $P < 0.01$;
270 Table 1). WUE estimations were most sensitive to the method of calculation on the hottest days
271 and during the heatwave (up to 91% difference within the same group; Table 1). Using the total
272 WUE_{day} , the significant difference in GPP did not translate to significantly different WUE_{day}
273 between the baseline and the driest days, which remained at $3 \text{ g C kg H}_2\text{O}^{-1}$ due to a comparable
274 decrease in ET during the driest days. In contrast, WUE_{day} decreased by 34% ($2.0 \pm 0.01 \text{ g C kg}$
275 H_2O^{-1}) on the hottest days and by 42% ($1.77 \pm 0.05 \text{ g C kg H}_2\text{O}^{-1}$) during the heatwave, which
276 resulted in significantly lower WUE during hot days than on the driest and baseline days. However,
277 the opposite trend occurred when accounting for the non-linear relationship between $\text{GPP} \times \text{VPD}$

278 and ET at the ecosystem scale; that is, the underlying WUE_{u_day} increased by 24% during the driest
279 days ($P < 0.01$; Table 1). Increasing WUE relative to baseline days was even more evident when
280 based on the intrinsic WUE_{i_day} , which increased by 30% during the driest days and by up to 125%
281 during the hottest days and heatwave ($P < 0.01$; Table 1), indicating that carbon assimilation
282 (approximated as GPP) per unit stomatal conductance (approximated as G_c) significantly
283 increased during high temperatures and high VPD, a result that was not captured when using total
284 WUE_{day} .

285 **Table 1.** Overview of the key response and climate variables for baseline days, the hottest and the
286 driest days, and during the heatwave. Values are mean daily sums and standard errors of water loss
287 as sap velocity (v_{sap_sum}) for both species and as ecosystem-scale evapotranspiration (ET_{sum}) and
288 potential ET (PET_{EBC_sum}), as well as daily gross primary productivity (GPP_{sum}), ecosystem
289 respiration (ER_{sum}), net ecosystem exchange (NEE_{sum}), mean daytime canopy conductance
290 (G_{cEBC_day}), water use efficiency (WUE_{day}), underlying WUE ($WUE_{u_day} = GPP \times VPD^{0.5} / ET$) and
291 intrinsic WUE ($WUE_{i_day} = GPP / G_c$), in addition to daily maximum vapor pressure deficit
292 (VPD_{max}) and temperature (T_{max}), and daily mean soil water content (Swc_{mean}) and incoming solar
293 radiation (F_{sd_mean}). Note that the subscript 'EBC' indicates that the available energy was set equal
294 to the sum of the latent and sensible heat flux to account for the energy imbalance when inverting
295 the Penman-Monteith combination equation to calculate canopy conductance and potential
296 evapotranspiration. Different superscript letters indicate significant differences among the groups
297 of days ($P < 0.05$, Tukey posthoc test).

	Baseline	Driest days	Hottest days	Heatwave
V_{sap_sum} <i>E. obliqua</i> (cm d ⁻¹)	597.6 ± 25.0 ^a	564.4 ± 23.3 ^a	867.9 ± 24.3 ^b	1017.1 ± 11.8 ^b
V_{sap_sum} <i>E. rubida</i> (cm d ⁻¹)	685.4 ± 32.6 ^a	717.6 ± 33.9 ^a	1083.7 ± 30.9 ^b	1281.5 ± 22.8 ^b
ET_{sum} (mm d ⁻¹)	2.88 ± 0.13 ^a	2.43 ± 0.15 ^a	4.12 ± 0.13 ^b	5.02 ± 0.16 ^b
PET_{EBC_sum} (mm d ⁻¹)	3.01 ± 0.20 ^a	3.91 ± 0.43 ^a	8.32 ± 0.38 ^b	9.62 ± 0.32 ^b
GPP_{sum} (g C d ⁻¹)	8.71 ± 0.28 ^b	7.3 ± 0.21 ^a	8.25 ± 0.22 ^{ab}	8.86 ± 0.32 ^{ab}
ER_{sum} (g C d ⁻¹)	4.07 ± 0.22 ^a	5.55 ± 0.36 ^b	7.85 ± 0.29 ^c	9.66 ± 0.31 ^c
NEE_{sum} (g C d ⁻¹)	-4.64 ± 0.34 ^a	-1.75 ± 0.48 ^b	-0.39 ± 0.37 ^b	0.79 ± 0.47 ^b
G_CEBC_{day} (mol m ⁻² s ⁻¹)	0.48 ± 0.002 ^c	0.27 ± 0.004 ^b	0.14 ± 0.003 ^a	0.15 ± 0.008 ^a
WUE_{day} (gC kgH ₂ O ⁻¹)	3.02 ± 0.02 ^b	3.01 ± 0.06 ^b	2.0 ± 0.01 ^a	1.77 ± 0.05 ^a
WUE_{u_day} (gC kPa ^{-0.5} kgH ₂ O ⁻¹)	2.64 ± 0.02 ^a	3.27 ± 0.06 ^b	3.09 ± 0.03 ^{ab}	3.02 ± 0.08 ^{ab}
WUE_{i_day} (gC mol ⁻¹ m ² s ⁻¹)	2.11 ± 0.02 ^a	2.74 ± 0.07 ^a	4.51 ± 0.05 ^b	4.74 ± 0.07 ^b
VPD_{max} (kPa)	1.4 ± 0.1 ^a	1.93 ± 0.18 ^a	4.22 ± 0.15 ^b	4.56 ± 0.29 ^b
T_{max} (°C)	20.6 ± 0.7 ^a	24.2 ± 0.9 ^b	33.4 ± 0.4 ^c	35.3 ± 0.8 ^c
SWC_{40cm_mean} (m ³ m ⁻³)	0.14 ± 0.002 ^b	0.1 ± 0.003 ^a	0.13 ± 0.003 ^{ab}	0.14 ± 0.001 ^b
Fsd_{mean} (W m ⁻²)	304.0 ± 11.6 ^a	303.2 ± 13.4 ^a	351.2 ± 7.3 ^a	322.6 ± 21.1 ^a

299 3.2 The diurnal cycle in response to increasing VPD

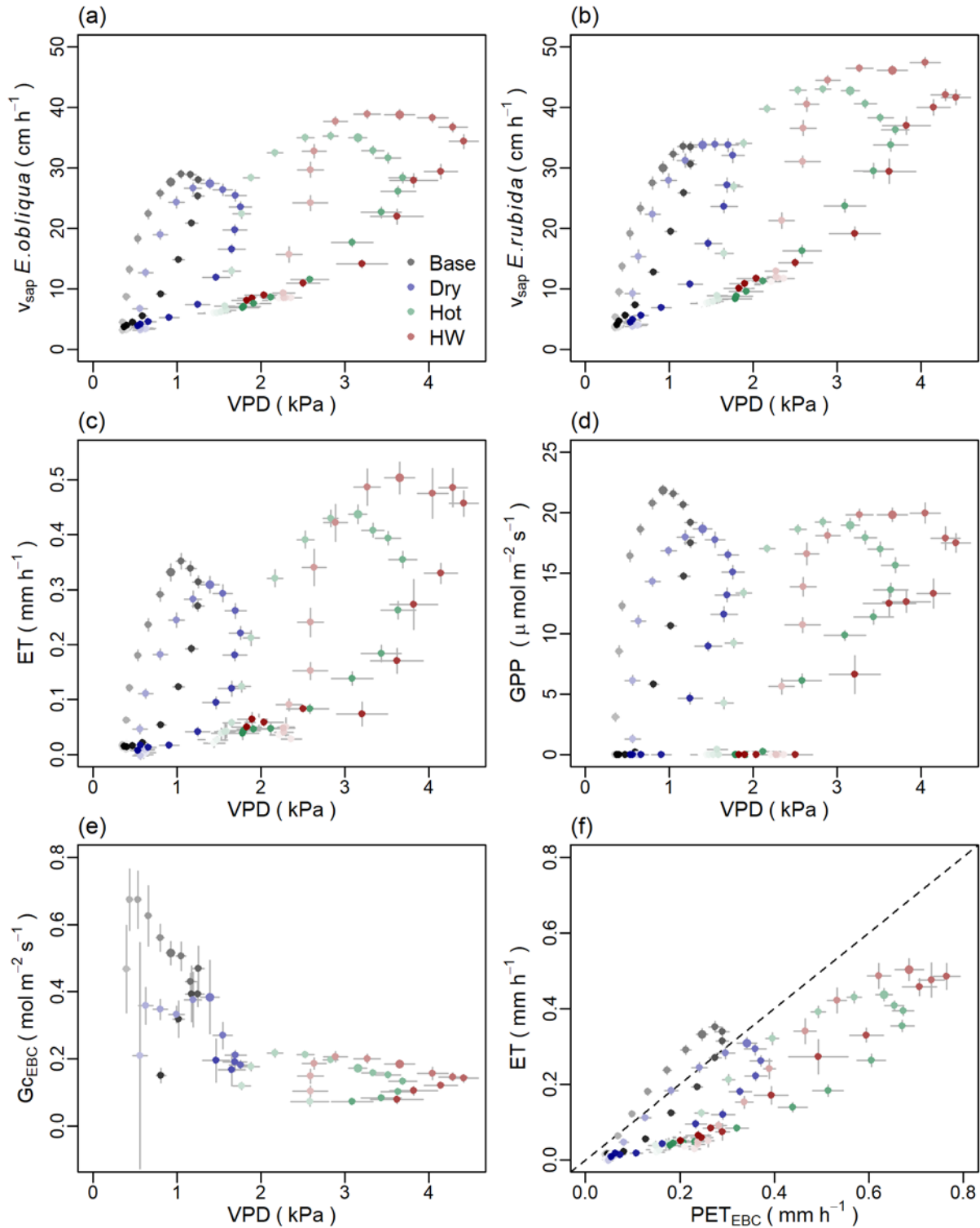
300 To further assess photosynthesis and water use during summer, we compared diurnal courses of
301 Gc, GPP, v_{sap} and ET as a function of VPD (Fig. 2a-e). On the hottest days, maximum v_{sap}
302 increased significantly (by 22% for *E. obliqua* and 28% for *E. rubida*; $P < 0.01$) compared with
303 baseline days, and v_{sap} remained at these elevated levels while VPD was between 2.6 and 3.2 kPa.
304 Thereafter, as VPD increased to 3.7 kPa in the mid-afternoon, v_{sap} decreased by 20% for *E. obliqua*
305 and 16% for *E. rubida* (i.e. equal to the maximum v_{sap} on baseline days). v_{sap} rates peaked during
306 the heatwave (39 cm h^{-1} for *E. obliqua* and 47.4 cm h^{-1} for *E. rubida*) and remained at these
307 significantly elevated levels (34% for *E. obliqua* and 42% for *E. rubida* above their baseline
308 maximum; $P < 0.01$) until VPD exceeded 4.3 kPa. In contrast, on the driest days, increasing VPD
309 decreased the peak v_{sap} of *E. obliqua* by 5%, while the peak v_{sap} for *E. rubida* remained comparable
310 to the baseline maximum (Fig. 2a, b). Apart from this small deviation on the driest days, both
311 species had a similar response to changes in VPD.

312 Consistent with v_{sap} dynamics, maximum ET at the ecosystem scale increased 24% on the hottest
313 days and by 43% during the heatwave (Fig. 2c; $P < 0.05$ for the heatwave). However, despite only
314 minor or no reductions in maximum v_{sap} on the driest days, maximum ET decreased by 12% on
315 the driest days relative to the summer baseline (Fig. 2c). As VPD increased in the afternoon, ET
316 decreased between 9 to 28% until maximum VPD was reached during all conditions. Overall, ET
317 dynamics were similar to v_{sap} dynamics, but more closely resembled the dynamics of *E. obliqua*
318 than *E. rubida* due the decrease of ET with increasing VPD during the driest days.

319 In contrast to significant increases in peak v_{sap} and ET during the hottest days and the heatwave,
320 the diurnal maximum of GPP declined with increasing VPD (Fig. 2d) and concurrently decreasing
321 Gc (Fig. 2e) under both hot and dry conditions relative to the summer baseline (by 12% and 15%

322 on the hottest and driest days, $P < 0.01$; and by 9% during the heatwave, $P > 0.05$; Fig. 2d). Until
323 maximum VPD was reached in the mid-afternoon, GPP decreased between 12 to 19% during all
324 conditions (Fig. 2d). While reductions of peak GPP were comparable to reductions of peak ET
325 during driest days (both decreased by 12%), the diurnal course of GPP and ET reversed during the
326 heatwave: mid-day GPP was sustained within 9% of baseline days ($P > 0.05$) at the cost of
327 significantly increased peak ET (43% increase compared to the summer baseline, $P < 0.05$).

328 Daytime canopy conductance varied considerably between the hottest, driest and baseline days
329 (Fig. 2e): maximum G_c at baseline days was $0.67 \text{ mol m}^{-2} \text{ s}^{-1}$, which decreased by 43% and 68%
330 on the driest and hottest days (to 0.38 and $0.22 \text{ mol m}^{-2} \text{ s}^{-1}$, respectively). Maximum G_c was
331 comparable between hot days and the heatwave, despite a larger VPD range during the heatwave
332 (Fig. 2e). However, G_c did not fully decline under any conditions, and the large reductions of G_c
333 on the driest, and especially on the hottest days and during the heatwave (Fig. 2e) only marginally
334 affected GPP (Fig. 2d). Consequently, reductions in G_c primarily restricted excessive water loss
335 during warm days with high atmospheric demand, which is supported by the ~50% reduction of
336 ET compared to PET (Fig. 2f and Table 1) during the hottest days and during the heatwave. In
337 addition, the close resemblance of diurnal ET and PET dynamics on the baseline and driest days
338 indicate that the forest was only marginally water limited on these days (Fig. 2f).



339

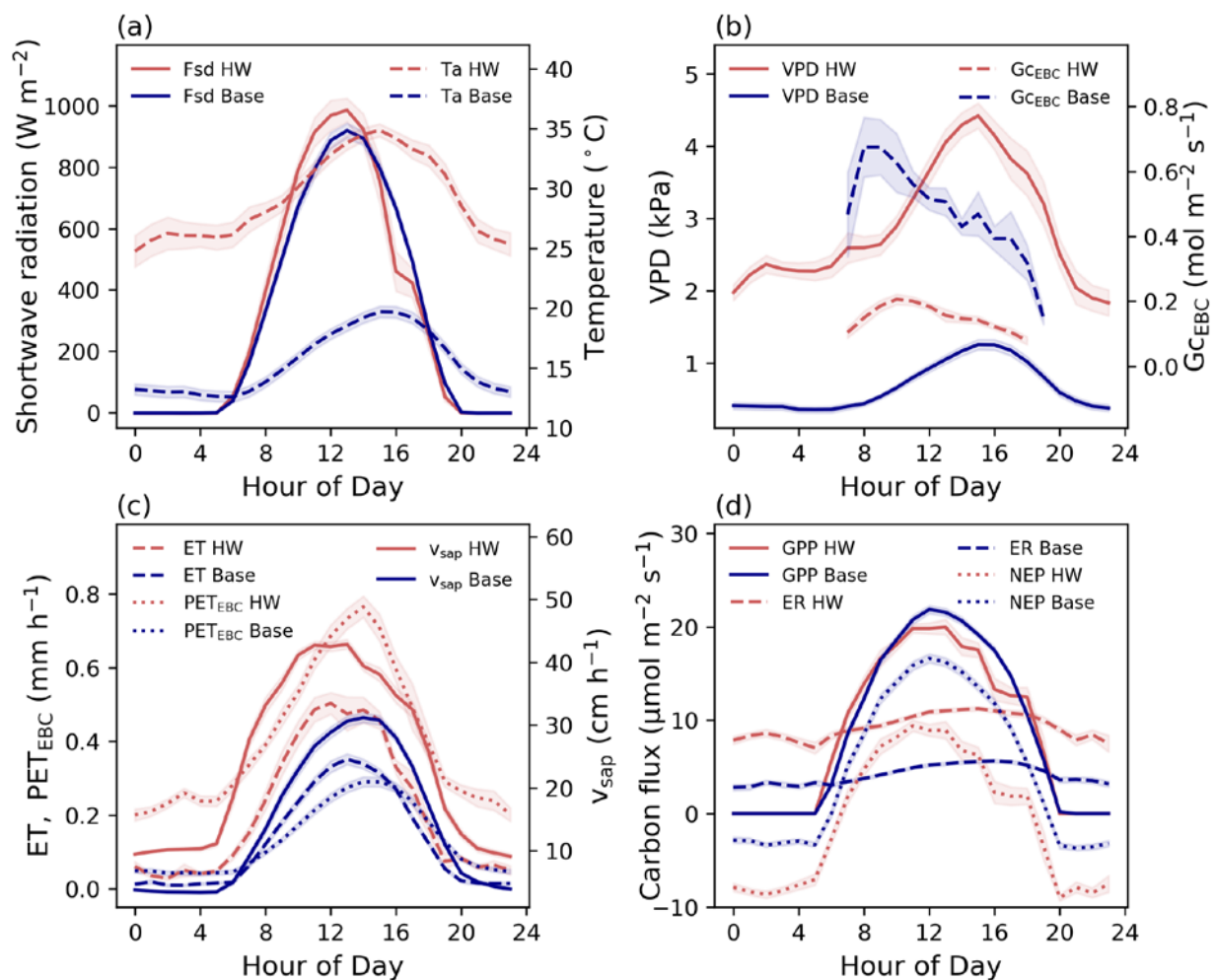
340 **Figure 2.** Diurnal patterns (means \pm standard error) of sap velocity (v_{sap} , cm h⁻¹),
341 evapotranspiration (ET, mm h⁻¹), gross primary productivity (GPP, $\mu\text{mol m}^{-2} \text{s}^{-1}$), and daytime

342 canopy conductance (G_{EBC} , $\text{mol m}^{-2} \text{s}^{-1}$) in response to increasing vapor pressure deficit (VPD,
343 kPa; panel a-e) and of ET against potential evapotranspiration (PET_{EBC} , mm h^{-1} ; panel f) during
344 the heatwave ('HW', red circles; 13-17 January 2014) on the hottest days ('Hot', green circles; air
345 temperature > 30.7 °C), driest days ('Dry', blue circles; $\text{SWC} < 0.1 \text{ m}^3 \text{ m}^{-3}$) and baseline days
346 ('Base', gray circles; January 2013, 2014 and 2015, excluding a hot period in January 2013, the
347 January 2014 heatwave, and the hottest and driest days). Note that the subscript 'EBC' indicates
348 that we set the available energy equal to the sum of the latent and sensible heat flux to account for
349 the energy imbalance when inverting the Penman-Monteith combination equation to calculate
350 canopy conductance and potential evapotranspiration. Symbols are colored according to the time
351 of day (hourly time steps, shades darken with progression of the day) and the highlighted symbol
352 indicates noon.

353 3.3 Carbon and water fluxes during a heat wave

354 The mean conditions during the five-day 2014 heatwave (13 to 17 January) compared with the
355 local baseline for January 2013, 2014 and 2015 were characterized by similar soil moisture content
356 ($0.13\text{-}0.21 \text{ m}^3 \text{ m}^{-3}$ during the baseline and $0.13\text{-}0.19 \text{ m}^3 \text{ m}^{-3}$ during the heatwave), but by 7% higher
357 incoming radiation peak, markedly warmer minimum (11.5 °C above baseline) and maximum
358 temperatures (14.7 °C above baseline), and ~four-fold higher atmospheric dryness (VPD), which
359 peaked at ~ 4.6 kPa in the early afternoon during the heatwave (Fig. 3a-b and Table 1). These
360 increases in temperature and VPD resulted in a 37% increase in peak v_{sap} rates and a 70% increase
361 in total daily water use compared to baseline days (averaged across both species; Fig. 3c and Table
362 1). While peak PET increased three-fold during the heatwave, peak ET only increased by 43%
363 compared to baseline days (Fig. 3c), leading to a 74% increase in total daily ET (from 2.88 mm on
364 baseline days to 5.02 mm during the heat wave; Table 1). In contrast to increases in v_{sap} and ET,

365 the daily peaks and daily totals of GPP remained relatively unchanged during the heatwave,
 366 indicating that baseline photosynthesis was maintained during the heatwave at the cost of
 367 significantly increased transpiration (Table 1 and Fig. 3d). However, despite stable GPP, a
 368 doubling of peak respiration rates ($P < 0.05$) and a more than two-fold increase in daily ER ($P < 0.01$)
 369 turned the forest from a moderate net carbon sink during baseline days ($-4.64 \pm 0.34 \text{ g C d}^{-1}$) into
 370 a net carbon source ($0.79 \pm 0.47 \text{ g C d}^{-1}$) during the heatwave ($P < 0.01$; Fig. 3d and Table 1).



371
 372 **Figure 3.** The mean conditions during the heatwave (HW, 13-17 January 2014; red lines)
 373 compared with the local baseline (Base, mean of January 2013-2015 without a hot period in 2013,

374 the 2014 heatwave and the hottest and driest days; blue lines). Abbreviations: F_{sd} = shortwave
375 radiation ($W m^{-2}$), T_a = air temperature ($^{\circ}C$), VPD = vapor pressure deficit (kPa), G_{EBC_day} = mean
376 daytime canopy conductance ($mol m^{-2} s^{-1}$), v_{sap} = sap velocity ($cm h^{-1}$, average of *E. obliqua* and
377 *E. rubida*), ET = evapotranspiration ($mm h^{-1}$), PET_{EBC} = potential evapotranspiration ($mm h^{-1}$),
378 GPP = gross primary productivity ($\mu mol m^{-2} s^{-1}$), NEP = net ecosystem productivity ($\mu mol m^{-2} s^{-1}$),
379 ER = ecosystem respiration ($\mu mol m^{-2} s^{-1}$). Note that shading represents standard error, and the
380 subscript 'EBC' indicates that we set the available energy equal to the sum of the latent and
381 sensible heat flux to account for the energy imbalance when calculating PET.

382 **4 Discussion**

383 4.1 Increased water use to sustain photosynthesis during high temperatures

384 Contrary to our first hypothesis, photosynthesis and water use within this dry-sclerophyll eucalypt
385 forest were not always synchronous during summer, as we measured no significant change in
386 photosynthesis in contrast to significantly increased water use in daily sums (Table 1), in response
387 to increasing VPD (Fig. 2), and in diurnal patterns (Fig. 3) during the hottest days and during the
388 5-day heatwave. On the hottest days and during the heatwave, photosynthesis was more-or-less
389 sustained at the cost of >70% increased water loss relative to baseline days, which contrasted with
390 concurrent decreases in both GPP (16%) and ET (16%) on the driest days. While hot or dry
391 conditions resulted in decreased canopy conductance, this primarily restricted excessive water loss
392 due to high atmospheric demand, and only marginally affected the GPP of this temperate eucalypt
393 forest.

394 The ability to maintain photosynthesis across hot or dry conditions indicates a yield-focused
395 growth strategy of the local eucalypt species, where carbon gain through photosynthesis is

396 prioritized over a conservative water use; this could partly explain the high annual carbon
397 sequestration rates that have been reported for this forest in comparison with other temperate
398 eucalypt forests (Beringer et al., 2016; Griebel et al., 2017; Hinko-Najera et al., 2017). Moreover,
399 our findings demonstrate potential for temperate eucalypt forests growing in relatively mild, mesic
400 conditions similar to our study site (e.g. at elevation or on cold sheltered sites with sufficient
401 moisture supply) to maintain photosynthesis under future warmer climates, whereas eucalypt
402 forests in less favorable growing conditions will likely increase stomatal adjustment to levels that
403 adversely affect photosynthetic uptake (Drake et al., 2018; van Gorsel et al., 2016; Renchon et al.,
404 2018). However, a doubling of ecosystem respiration turned the forest from a moderate net carbon
405 sink into a net carbon source during the heatwave. Thus, while the photosynthesis of this eucalypt
406 forest appears largely unaffected during warmer and drier conditions in the summer months, the
407 over-proportional increase in ER resulted in a switch from a net sink to a source, highlighting that
408 the net productivity can be adversely affected by isolated extreme events. Hence, with a projected
409 increase in the number, duration and intensity of heat waves, the potential of temperate eucalypt
410 forests to remain carbon sinks under future climates will largely depend on the response of
411 ecosystem respiration to increasing temperatures rather than the ability to sustain photosynthesis
412 during extreme heat.

413 The large increase in ET during the hottest days and the heatwave resulted in up to two-fold
414 variations in total WUE in summer, with conflicting trends depending on the formulation of WUE
415 (Table 1). While seasonal variation in WUE within the same ecosystem is typically linked to
416 variations in canopy phenology (Huang et al., 2016; Jin et al., 2017), our observations were
417 constrained to the summer season and pooled across three different summers with similar radiation
418 input for all examined conditions (Fig. S1.), thereby minimizing phenological influences as well

419 as climatological variation. Yet, significant differences between the baseline and driest days in
420 underlying WUE indicated that this metric was more sensitive to capturing physiological responses
421 to drought stress than intrinsic WUE, possibly because WUE_{u_day} reduces large parts of the diurnal
422 and seasonal variation at the ecosystem scale within the same plant functional type (Zhou et al.,
423 2015). In contrast, WUE_{i_day} doubled during the hottest days and the heatwave, and accurately
424 captured the significantly increased rate of photosynthesis per unit conductance. Despite different
425 sensitivities of underlying and intrinsic WUE to either dry or hot conditions at our study site, none
426 of these physiological responses were captured using the traditional formulation of WUE
427 (GPP/ET), supporting that alternative formulations of WUE improved insights into the
428 mechanisms regulating water loss and carbon uptake.

429 4.2 Dependence on atmospheric demand

430 The influence of VPD on carbon and water fluxes has been well acknowledged (Beer et al., 2009;
431 Eamus et al., 2013; Knauer et al., 2015; Novick et al., 2016; Renchon et al., 2018), and short- and
432 long-term reductions in GPP and transpiration due to fluctuations in VPD and soil moisture have
433 been recorded across a range of biomes even during non-drought years (Sulman et al., 2016).
434 Further, a decrease in transpiration and photosynthesis due to stomatal regulation in response to
435 increasing VPD is well established for eucalypts (Duursma et al., 2014; Mitchell et al., 2012;
436 Pepper et al., 2008; Prior et al., 1997). While our study indicated that stomatal regulation of water
437 loss can differ between exceptionally hot conditions and dry conditions, ecosystem-scale estimates
438 of canopy conductance to infer stomatal activity are subject to large uncertainties as G_c is only
439 inferred and not directly measured (Knauer et al., 2015; Wohlfahrt et al., 2009). While we
440 attempted to minimize the contribution of non-transpirational water fluxes by removing rainy
441 periods and by forcing energy balance closure (section 2.3), stomatal regulation might still be

442 confounded by anatomical properties of water transport; that is, the v_{sap} to VPD response can vary
443 if the water absorption capacity at the root-soil interface becomes limiting or if the xylem anatomy
444 restricts the water transport capacity from the roots to the canopy (Eamus & Prior, 2001; Sperry &
445 Pockman, 1993; Tyree & Ewers, 1991). Still, ET was significantly reduced compared with PET on
446 the hottest days and during the heatwave, providing clear indications of physiological regulations
447 of water loss in response to increasing atmospheric demand in our forest, whereas the relative
448 importance of stomatal regulations versus hydraulic restrictions on water transport remains
449 unclear. Furthermore, the ability to maintain or even increase v_{sap} rates in all the conditions of our
450 study suggests that the trees likely had access to soil water in deeper layers (section 4.3). Despite
451 excluding rainy periods from our analyses, reduced peak rates and daily totals of ET on the driest
452 days were not clearly due to decreases in v_{sap} , indicating a greater relative contribution of soil and
453 canopy evaporation (or the lack thereof) to ecosystem-scale ET dynamics during dry conditions.
454 Nevertheless, ET dynamics closely resembled v_{sap} dynamics of *E. obliqua*, confirming that stand-
455 scale observations of ET were dominated by the transpiration dynamics of the dominating species
456 (70% of stand basal area; Griebel 2016).

457 4.3 Dependence on water availability

458 We can partially confirm our second hypothesis that evapotranspiration increases during a longer
459 heatwave, however GPP remained comparable to baseline days and we did not measure a
460 simultaneous sharp reduction in photosynthesis rates during the heatwave (as was measured for
461 one-year old eucalypt saplings by Drake et al., 2018). This suggests that temperature stress may
462 be ameliorated by water access at this comparatively mesic site. In addition to moderate moisture
463 levels down to 1 m depth during the heatwave (ranging from 0.13 to 0.19 $\text{m}^3 \text{m}^{-3}$), sustained v_{sap}
464 even during the driest days suggests that the trees had access to deep water reserves, which were

465 likely recharged in the 2010/2011 LaNiña years when annual rainfall totals were ~200-400 mm
466 above the long-term average. Eucalypts can have fast-growing roots that allow them to reach deep
467 water resources quickly (e.g. 12 m depth in 2 years; Christina et al., 2017), and deep soil water
468 access is known to be an important buffer in north Australia's open forests and savanna regions,
469 where large amounts of water stored during the wet season can be accessed by trees during dry
470 periods (Arndt et al., 2015; Eamus et al., 2015; Hutley et al., 2000; O'Grady et al., 1999). Even
471 for temperate eucalypt forests in more complex terrain, access to water in deep soil layers has
472 explained water losses that have exceeded annual precipitation inputs (Benyon & Doody, 2015;
473 Mitchell et al., 2012). Hence, while access to deep soil water might represent an efficient
474 adaptation of eucalypt trees to drought (Duursma et al., 2011; Markewitz et al., 2010; Nepstad et
475 al., 2007; Yang et al., 2017), our study indicates that deep soil water access also plays an important
476 role in explaining comparatively high carbon sequestration rates of temperate eucalypt forests.
477 Furthermore, we found no evidence that the forest was exposed to severe heat or drought stress
478 during our three observation years, which is supported by an absence of increased leaf shedding
479 (Griebel et al., 2015) - a typical stress response for eucalypts (Granda et al., 2014; Pook, 1984;
480 Renchon et al., 2018; Silva et al., 2004) - and by a sustained leaf area index whereby leaf loss was
481 consistently balanced by growth of new leaves in our forest (Griebel et al., 2017). In addition,
482 sustained photosynthetic rates during high temperatures indicate some buffer in the capacity of
483 this forest type to maintain productivity under a warming climate; however, effects on productivity
484 of very hot conditions combined with very dry conditions remain unclear, particularly if sustained
485 dry conditions lead to a depletion in deep soil water reserves.

486 **5 Conclusions**

487 We present evidence that this temperate eucalypt forest was able to sustain photosynthesis at the
488 cost of increased water loss during individual exceptionally hot days and during a longer heatwave,
489 which contradicted our hypotheses of (i) concomitant reductions or increases in transpiration and
490 photosynthesis, and (ii) notably decreasing photosynthesis with increasing transpiration during
491 heatwaves. Increased or sustained transpiration rates during the hottest, driest and heatwave days
492 indicated sufficient water availability to sustain photosynthesis rates at our study site, and
493 consequently that neither individual hot or dry days, nor the heat wave coincided with water deficit
494 and/or drought stress. This, in turn, indicated access of the roots to deeper water reserves. How
495 sustainable such water reserves are, and how much these reserves will be depleted by prolonged
496 heat waves or dry conditions remains unclear. Moreover, the switch from a net sink to a net source
497 of carbon during the heatwave highlights potential limitations to similar, high elevation temperate
498 eucalypt forests remaining carbon sinks under future climates, which will largely depend on the
499 response of ecosystem respiration to increasing temperatures rather than their potential to maintain
500 photosynthesis during hot or dry conditions.

501 **Acknowledgments**

502 We thank John Collopy and Julio Najera-Umana for assisting with the installation of the field
503 equipment. This study was partly funded by TERN-OzFlux and TERN-SuperSites, the Australian
504 Research Council (ARC) grants LE0882936 and DP120101735, and the Integrated Forest
505 Ecosystem Research program supported by the Victorian Department of Environment Land, Water
506 and Planning (DELWP). The flux tower data are available at the OzFlux portal
507 (<http://data.ozflux.org.au>) and the tree water use data are available at Sapfluxnet

508 (<http://sapfluxnet.creaf.cat/app>). We appreciate substantive input from four anonymous reviewers
509 which improved the quality of the manuscript.

510 **References**

- 511 Ameye, M., Wertin, T. M., Bauweraerts, I., McGuire, M. A., Teskey, R. O., & Steppe, K. (2012).
512 The effect of induced heat waves on *Pinus taeda* and *Quercus rubra* seedlings in ambient and
513 elevated CO₂ atmospheres. *New Phytologist*, *196*(2), 448–461.
- 514 Arndt, S. K., Sanders, G. J., Bristow, M., Hutley, L. B., Beringer, J., & Livesley, S. J. (2015).
515 Vulnerability of native savanna trees and exotic *Khaya senegalensis* to seasonal drought. *Tree*
516 *Physiology*, *35*(7), 783–791.
- 517 Ball, J. T., Woodrow, I. E., & Berry, J. A. (1987). A model predicting stomatal conductance and
518 its contribution to the control of photosynthesis under different environmental conditions. In
519 *Progress in photosynthesis research* (pp. 221–224). Springer.
- 520 Barr, A., Richardson, A., Hollinger, D., Papale, D., Arain, M., Black, T., et al. (2013). Use of
521 change-point detection for friction–velocity threshold evaluation in eddy-covariance studies.
522 *Agricultural and Forest Meteorology*, *171*, 31–45.
- 523 Beer, C., Ciais, P., Reichstein, M., Baldocchi, D., Law, B., Papale, D., Soussana, J., Ammann, C.,
524 Buchmann, N., Frank, D., 2009. Temporal and among-site variability of inherent water use
525 efficiency at the ecosystem level. *Global Biogeochemical Cycles* *23*.
- 526 Benyon, R. G., & Doody, T. M. (2015). Comparison of interception, forest floor evaporation and
527 transpiration in *Pinus radiata* and *Eucalyptus globulus* plantations. *Hydrological Processes*, *29*(6),
528 1173–1187.

- 529 Beringer, J., Hutley, L. B., McHugh, I., Arndt, S. K., Campbell, D., Cleugh, H. A., et al. (2016).
530 An introduction to the Australian and New Zealand flux tower network - OzFlux. *Biogeosciences*,
531 *13*(21), 5895–5916.
- 532 Breshears, D. D., Adams, H. D., Eamus, D., McDowell, N., Law, D. J., Will, R. E., et al. (2013).
533 The critical amplifying role of increasing atmospheric moisture demand on tree mortality and
534 associated regional die-off. *Frontiers in Plant Science*, *4*, 266.
- 535 Brouwers, N. C., Mercer, J., Lyons, T., Poot, P., Veneklaas, E., & Hardy, G. (2013). Climate and
536 landscape drivers of tree decline in a Mediterranean ecoregion. *Ecology and Evolution*, *3*(1), 67–
537 79.
- 538 Bureau of Meteorology (2013). *Special Climate Statement 43 – extreme heat in January 2013*.
539 (BOM Publication No. SCS-43). Retrieved from
540 <http://www.bom.gov.au/climate/current/statements/scs43e.pdf>
- 541 Bureau of Meteorology (2014). *Special Climate Statement 48 – one of southeast Australia’s most*
542 *significant heatwaves*. (BOM Publication No. SCS-48). Retrieved from
543 <http://www.bom.gov.au/climate/current/statements/scs48.pdf>
- 544 Bureau of Meteorology (2015). *Annual climate statement 2015*. Retrieved from
545 <http://www.bom.gov.au/climate/current/annual/aus/2015/>.
- 546 Bureau of Meteorology (2016a). *Annual climate statement 2016*. Retrieved from
547 <http://www.bom.gov.au/climate/current/annual/aus/2016/>.
- 548 Bureau of Meteorology (2016b). *Drought Statement - April rainfall reduces deficiencies in some*
549 *areas*. Retrieved from <http://www.bom.gov.au/climate/drought/archive/20160505.shtml>.

- 550 Choat, B., Jansen, S., Brodribb, T. J., Cochard, H., Delzon, S., Bhaskar, R., et al. (2012). Global
551 convergence in the vulnerability of forests to drought. *Nature*, 491(7426), 752.
- 552 Christina, M., Nouvellon, Y., Laclau, J. P., Stape, J. L., Bouillet, J. P., Lambais, G. R., & Maire,
553 G. le. (2017). Importance of deep water uptake in tropical eucalypt forest. *Functional Ecology*,
554 31(2), 509–519.
- 555 Cowan, I. (1978). Stomatal behaviour and environment. In *Advances in botanical research* (Vol.
556 4, pp. 117–228). Elsevier.
- 557 De Kauwe, M.G., Medlyn, B.E., Pitman, A.J., Drake, J.E., Ukkola, A., Griebel, A. et al. (2019).
558 Examining the evidence for decoupling between photosynthesis and transpiration during heat
559 extremes. *Biogeosciences* 16, 903–916.
- 560 Drake, J. E., Tjoelker, M. G., Vårhammar, A., Medlyn, B. E., Reich, P. B., Leigh, A., et al. (2018).
561 Trees tolerate an extreme heatwave via sustained transpirational cooling and increased leaf thermal
562 tolerance. *Global Change Biology*. DOI: 10.1111/gcb.14037
- 563 Duursma, R. A., Barton, C. V. M., Eamus, D., Medlyn, B. E., Ellsworth, D. S., Forster, M. A., et
564 al. (2011). Rooting depth explains CO₂ x drought interaction in *Eucalyptus saligna*. *Tree*
565 *Physiology*, 31(9), 922–931.
- 566 Duursma, R. A., Barton, C. V. M., Lin, Y. S., Medlyn, B. E., Eamus, D., Tissue, D. T., et al.
567 (2014). The peaked response of transpiration rate to vapour pressure deficit in field conditions can
568 be explained by the temperature optimum of photosynthesis. *Agricultural and Forest Meteorology*,
569 189, 2–10.
- 570 Eamus, D., & Prior, L. (2001). Ecophysiology of trees of seasonally dry tropics: Comparisons
571 among phenologies. *Australian Journal of Botany*, 32, 113–197.

- 572 Eamus, D., Taylor, D. T., Macinnis-Ng, C. M., Shanahan, S., & De Silva, L. (2008). Comparing
573 model predictions and experimental data for the response of stomatal conductance and guard cell
574 turgor to manipulations of cuticular conductance, leaf-to-air vapour pressure difference and
575 temperature: Feedback mechanisms are able to account for all observations. *Plant, Cell &*
576 *Environment*, 31(3), 269–277.
- 577 Eamus, D., Boulain, N., Cleverly, J., & Breshears, D. D. (2013). Global change-type drought-
578 induced tree mortality: Vapor pressure deficit is more important than temperature per se in causing
579 decline in tree health. *Ecology and Evolution*, 3(8), 2711–2729.
- 580 Eamus, D., Zolfaghar, S., Villalobos-Vega, R., Cleverly, J., & Huete, A. (2015). Groundwater-
581 dependent ecosystems: Recent insights from satellite and field-based studies. *Hydrology and Earth*
582 *System Sciences*, 19(10), 4229–4256.
- 583 Farquhar, G. D., & Sharkey, T. D. (1982). Stomatal conductance and photosynthesis. *Annual*
584 *Review of Plant Physiology*, 33(1), 317–345.
- 585 van Gorsel, E., Wolf, S., Cleverly, J., Isaac, P., Haverd, V., Ewenz, C., et al. (2016). Carbon uptake
586 and water use in woodlands and forests in southern Australia during an extreme heat wave event
587 in the “Angry summer” of 2012/2013. *Biogeosciences*, 13(21), 5947–5964.
- 588 Granda, V., Delatorre, C., Cuesta, C., Centeno, M. L., Fernández, B., Rodríguez, A., & Feito, I.
589 (2014). Physiological and biochemical responses to severe drought stress of nine *Eucalyptus*
590 *globulus* clones: A multivariate approach. *Tree Physiology*, 34(7), 778–786.
- 591 Griebel, A., Bennett, L. T., Culvenor, D. S., Newnham, G. J., & Arndt, S. K. (2015). Reliability
592 and limitations of a novel terrestrial laser scanner for daily monitoring of forest canopy dynamics.
593 *Remote Sensing of Environment*, 166, 205–213.

- 594 Griebel, A. (2016). New approaches to investigate the seasonal growth dynamics in forests,
595 (Doctoral dissertation). Retrieved from Minerva Access. (<http://hdl.handle.net/11343/112613>).
596 Melbourne, Australia: The University of Melbourne.
- 597 Griebel, A., Bennett, L. T., Metzen, D., Cleverly, J., Burba, G., & Arndt, S. K. (2016). Effects of
598 inhomogeneities within the flux footprint on the interpretation of seasonal, annual, and interannual
599 ecosystem carbon exchange. *Agricultural and Forest Meteorology*, 221, 50-60.
- 600 Griebel, A., Bennett, L. T., & Arndt, S. K. (2017). Evergreen and ever growing - stem and canopy
601 growth dynamics of a temperate eucalypt forest. *Forest Ecology and Management*, 389, 417–426.
- 602 Hinko-Najera, N., Isaac, P., Beringer, J., Gorsel, E. van, Ewenz, C., McHugh, I., et al. (2017). Net
603 ecosystem carbon exchange of a dry temperate eucalypt forest. *Biogeosciences*, 14(16), 3781–
604 3800.
- 605 Huang, M. T., Piao, S. L., Zeng, Z. Z., Peng, S. S., Ciais, P., Cheng, L., et al. (2016). Seasonal
606 responses of terrestrial ecosystem water-use efficiency to climate change. *Global Change Biology*,
607 22(6), 2165–2177.
- 608 Hughes, L., Cawsey, E., & Westoby, M. (1996). Climatic range sizes of Eucalyptus species in
609 relation to future climate change. *Global Ecology and Biogeography Letters*, 23–29.
- 610 Hutley, L. B., O’Grady, A. P., & Eamus, D. (2000). Evapotranspiration from eucalypt open-forest
611 Savanna of northern Australia. *Functional Ecology*, 14(2), 183–194.
- 612 Isaac, P., Cleverly, J., McHugh, I., Gorsel, E. van, Ewenz, C., & Beringer, J. (2017). OzFlux data:
613 Network integration from collection to curation. *Biogeosciences*, 14(12), 2903–2928.

- 614 Jin, J., Zhan, W., Wang, Y., Gu, B., Wang, W., Jiang, H., et al. (2017). Water use efficiency in
615 response to interannual variations in flux-based photosynthetic onset in temperate deciduous
616 broadleaf forests. *Ecological Indicators*, 79(Supplement C), 122–127.
- 617 Jurskis, V. (2005). Eucalypt decline in Australia, and a general concept of tree decline and dieback.
618 *Forest Ecology and Management*, 215(1–3), 1–20.
- 619 Knauer, J., Werner, C. & Zaehle, S. (2015). Evaluating stomatal models and their atmospheric
620 drought response in a land surface scheme: A multibiome analysis. *Journal of Geophysical*
621 *Research: Biogeosciences* 120, 1894–1911.
- 622 Knauer, J., Zaehle, S., Medlyn, B.E., Reichstein, M., Williams, C.A., Migliavacca, M. et al. (2018).
623 Towards physiologically meaningful water-use efficiency estimates from eddy covariance data.
624 *Global Change Biology* 24, 694–710.
- 625 Leuning, R. (1995). A critical appraisal of a combined stomatal-photosynthesis model for C3
626 plants. *Plant, Cell & Environment*, 18(4), 339–355.
- 627 Markewitz, D., Devine, S., Davidson, E. A., Brando, P., & Nepstad, D. C. (2010). Soil moisture
628 depletion under simulated drought in the Amazon: Impacts on deep root uptake. *New Phytologist*,
629 187(3), 592–607.
- 630 Matusick, G., Ruthrof, K. X., Brouwers, N. C., Dell, B., & Hardy, G. S. J. (2013). Sudden forest
631 canopy collapse corresponding with extreme drought and heat in a mediterranean-type eucalypt
632 forest in southwestern Australia. *European Journal of Forest Research*, 132(3), 497–510.
- 633 McDowell, N., Pockman, W. T., Allen, C. D., Breshears, D. D., Cobb, N., Kolb, T., et al. (2008).
634 Mechanisms of plant survival and mortality during drought: Why do some plants survive while
635 others succumb to drought? *New Phytologist*, 178(4), 719–739.

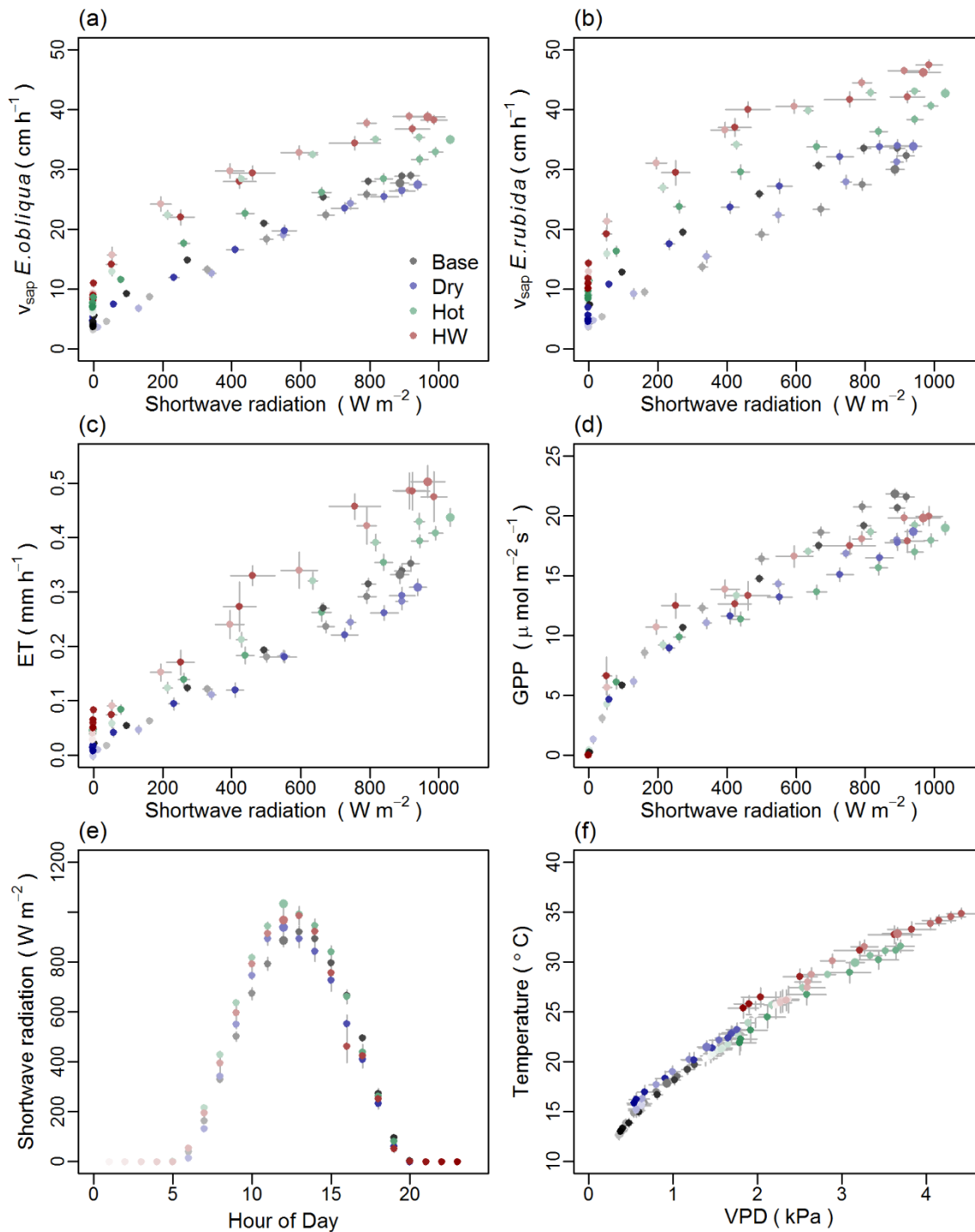
- 636 McDowell, N. G. (2011). Mechanisms linking drought, hydraulics, carbon metabolism, and
637 vegetation mortality. *Plant Physiology*, *155*(3), 1051–1059.
- 638 Medlyn, B. E., Duursma, R. A., Eamus, D., Ellsworth, D. S., Prentice, I. C., Barton, C. V., et al.
639 (2011). Reconciling the optimal and empirical approaches to modelling stomatal conductance.
640 *Global Change Biology*, *17*(6), 2134–2144.
- 641 Mitchell, P. J., Benyon, R. G., & Lane, P. N. J. (2012). Responses of evapotranspiration at different
642 topographic positions and catchment water balance following a pronounced drought in a mixed
643 species eucalypt forest, Australia. *Journal of Hydrology*, *440*, 62–74.
- 644 Mitchell, P. J., O’Grady, A. P., Hayes, K. R., & Pinkard, E. A. (2014a). Exposure of trees to
645 drought-induced die-off is defined by a common climatic threshold across different vegetation
646 types. *Ecology and Evolution*, *4*(7), 1088–1101.
- 647 Mitchell, P. J., O’Grady, A. P., Tissue, D. T., Worledge, D., & Pinkard, E. A. (2014b). Co-
648 ordination of growth, gas exchange and hydraulics define the carbon safety margin in tree species
649 with contrasting drought strategies. *Tree Physiology*, *34*(5), 443–458.
- 650 Monteith, J. L. (1965). Evaporation and environment. *Symposium of the Society for Experimental*
651 *Biology*, *19*, 205–224.
- 652 Nepstad, D. C., Tohver, I. M., Ray, D., Moutinho, P., & Cardinot, G. (2007). Mortality of large
653 trees and lianas following experimental drought in an Amazon forest. *Ecology*, *88*(9), 2259–2269.
- 654 Novick, K. A., Ficklin, D. L., Stoy, P. C., Williams, C. A., Bohrer, G., Oishi, A. C., et al. (2016).
655 The increasing importance of atmospheric demand for ecosystem water and carbon fluxes. *Nature*
656 *Climate Change*.

- 657 O'Grady, A. P., Eamus, D., & Hutley, L. B. (1999). Transpiration increases during the dry season:
658 Patterns of tree water use in eucalypt open-forests of northern Australia. *Tree Physiology*, *19*(9),
659 591–597.
- 660 Pepper, D. A., McMurtrie, R. E., Medlyn, B. E., Keith, H., & Eamus, D. (2008). Mechanisms
661 linking plant productivity and water status for a temperate eucalyptus forest flux site: Analysis
662 over wet and dry years with a simple model. *Functional Plant Biology*, *35*(6), 493–508.
- 663 Pook, E. W. (1984). Canopy dynamics of *Eucalyptus-maculata* Hook .1. Distribution and
664 dynamics of leaf populations. *Australian Journal of Botany*, *32*(4), 387–403.
- 665 Prior, L. D., Eamus, D., & Duff, G. A. (1997). Seasonal and diurnal patterns of carbon assimilation,
666 stomatal conductance and leaf water potential in *Eucalyptus tetradonta* saplings in a wet-dry
667 savanna in northern Australia. *Australian Journal of Botany*, *45*(2), 241–258.
- 668 R Core Team. (2018). *R: A language and environment for statistical computing*. Vienna, Austria:
669 R Foundation for Statistical Computing. Retrieved from <https://www.R-project.org/>
- 670 Renchon, A. A., Griebel, A., Metzen, D., Williams, C. A., Medlyn, B., Duursma, R. A., et al.
671 (2018). Upside-down fluxes Down Under: CO₂ net sink in winter and net source in summer in a
672 temperate evergreen broadleaf forest. *Biogeosciences*, *15*(12), 3703-3716.
- 673 Schulze, E.-D. & Hall, A. (1982). Stomatal responses, water loss and CO₂ assimilation rates of
674 plants in contrasting environments, in: *Physiological Plant Ecology I*. Springer, pp. 181–230.
- 675 Silva, F. C. e, Shvaleva, A., Maroco, J., Almeida, M., Chaves, M., & Pereira, J. (2004). Responses
676 to water stress in two *Eucalyptus globulus* clones differing in drought tolerance. *Tree Physiology*,
677 *24*(10), 1165–1172.

- 678 Smith, D. M., Larson, B. C., Kelty, M. J., & Ashton, P. M. S. (1997). *The practice of silviculture:*
679 *Applied forest ecology*. Book, John Wiley; Sons, Inc.
- 680 Sperry, J., & Pockman, W. (1993). Limitation of transpiration by hydraulic conductance and xylem
681 cavitation in *Betula occidentalis*. *Plant, Cell & Environment*, 16(3), 279–287.
- 682 Sulman, B. N., Roman, D. T., Yi, K., Wang, L. X., Phillips, R. P., & Novick, K. A. (2016). High
683 atmospheric demand for water can limit forest carbon uptake and transpiration as severely as dry
684 soil. *Geophysical Research Letters*, 43(18), 9686–9695.
- 685 Teuling, A.J., Seneviratne, S.I., Stöckli, R., Reichstein, M., Moors, E., Ciais, P. et al. (2010).
686 Contrasting response of European forest and grassland energy exchange to heatwaves. *Nature*
687 *Geoscience* 3, 722.
- 688 Thomas, D., & Eamus, D. (1999). The influence of predawn leaf water potential on stomatal
689 responses to atmospheric water content at constant c_i and on stem hydraulic conductance and foliar
690 abscisic acid concentrations. *Journal of Experimental Botany*, 50(331), 243–251.
- 691 Tuzet, A., Perrier, A., & Leuning, R. (2003). A coupled model of stomatal conductance,
692 photosynthesis and transpiration. *Plant, Cell & Environment*, 26(7), 1097–1116.
- 693 Tyree, M. T., & Sperry, J. S. (1989). Vulnerability of xylem to cavitation and embolism. *Annual*
694 *Review of Plant Biology*, 40(1), 19–36.
- 695 Tyree, M. T., & Ewers, F. W. (1991). The hydraulic architecture of trees and other woody plants.
696 *New Phytologist*, 119(3), 345–360.
- 697 Urban, J., Ingwers, M. W., McGuire, M. A., & Teskey, R. O. (2017). Increase in leaf temperature
698 opens stomata and decouples net photosynthesis from stomatal conductance in *Pinus taeda* and
699 *Populus deltoides* x *nigra*. *Journal of Experimental Botany*, 68(7), 1757–1767.

- 700 Webb, E. K., Pearman, G. I., & Leuning, R. (1980). Correction of flux measurements for density
701 effects due to heat and water-vapor transfer. *Quarterly Journal of the Royal Meteorological*
702 *Society*, 106(447), 85–100.
- 703 Whitehead, D., & Beadle, C. L. (2004). Physiological regulation of productivity and water use in
704 Eucalyptus: A review. *Forest Ecology and Management*, 193(1), 113–140.
- 705 Wilson, K., Goldstein, A., Falge, E., Aubinet, M., Baldocchi, D., Berbigier, P. et al. (2002). Energy
706 balance closure at Fluxnet sites. *Agricultural and Forest Meteorology* 113, 223–243.
- 707 Wohlfahrt, G., Haslwanter, A., Hortnagl, L., Jasoni, R.L., Fenstermaker, L.F., Arnone, 3., J. A. &
708 Hammerle, A. (2009). On the consequences of the energy imbalance for calculating surface
709 conductance to water vapour. *Agricultural and Forest Meteorology* 149, 1556–1559.
- 710 Yang, F. T., Feng, Z. M., Wang, H. M., Dai, X. Q., & Fu, X. L. (2017). Deep soil water extraction
711 helps to drought avoidance but shallow soil water uptake during dry season controls the inter-
712 annual variation in tree growth in four subtropical plantations. *Agricultural and Forest*
713 *Meteorology*, 234, 106–114
- 714 Zhou, S., Yu, B., Huang, Y., & Wang, G. (2014). The effect of vapor pressure deficit on water use
715 efficiency at the subdaily time scale. *Geophysical Research Letters* 41, 5005–5013.
- 716 Zhou, S., Yu, B., Huang, Y. & Wang, G. (2015). Daily underlying water use efficiency for
717 Ameriflux sites. *Journal of Geophysical Research: Biogeosciences* 120, 887–902.

718 **Supporting Information**



719

720 **Figure S1.** Diurnal patterns (means \pm standard error) of sap velocity (v_{sap} , $cm h^{-1}$),

721 evapotranspiration (ET, $mm h^{-1}$), gross primary productivity (GPP, $\mu mol m^{-2} s^{-1}$) against solar

722 radiation (Shortwave radiation, W m^{-2} ; panel a-d), as well as the diurnal course of shortwave
723 radiation (panel e) and of VPD against air temperature ($^{\circ}\text{C}$; panel f) during the heatwave ('HW',
724 red circles; 13-17 January 2014) on the hottest days ('Hot', green circles; air temperature > 30.7
725 $^{\circ}\text{C}$), driest days ('Dry', blue circles; $\text{SWC} < 0.1 \text{ m}^3 \text{ m}^{-3}$) and baseline days ('Base', gray circles;
726 January 2013, 2014 and 2015, excluding a hot period in January 2013, the January 2014 heatwave,
727 and the hottest and driest days). Symbols are colored according to the time of day (hourly time
728 steps, shades darken with progression of the day) and the highlighted symbol indicates noon.